#6172

NUMERICAL COMPUTATION OF FLOW AND HEAT TRANSFER IN AIR-CONDITIONED ROOMS BY A SPECIAL VELOCITY-PRESSURE ITERATION AND A MULTIGRID METHOD[†]

Markus Rösler and Bernd Hanel
Dresden University of Technology
Dresden, Germany

SUMMARY

Starting from the basic equations for the calculation of turbulent flows a velocity–pressure iteration is presented. Main part of this algorithm is a Poisson equation for pressure. A multigrid method is applied to solve this equation.

The strategy was used to investigate laminar as well as turbulent flows in ventilated rooms. For a laminar nonisothermal flow a comparison is given between a coupled and a uncoupled solution on two grids concerning number of time steps, maximal velocity, contraction rate of the multigrid solver and mean Nußelt number. Furthermore, two isothermal turbulent flow situations were simulated. For the test case 2D1 specified by *Nielsen (1990)* 2D and 3D simulations were carried out and evaluated. A similar situation, which was investigated by own experiments, was calculated and compared in terms of agreement with the measurement and influence of numerical parameters.

Simulations were carried out by a research code developed by the authors and their co–workers on workstations under UNIX.

[†]The research was supported by the Bundesministerium für Forschung und Technologie under the contract 0329016D.

NUMERICAL COMPUTATION OF FLOW AND HEAT TRANSFER IN AIR-CONDITIONED ROOMS BY A SPECIAL VELOCITY-PRESSURE ITERATION AND A MULTIGRID METHOD

Markus Rösler and Bernd Hanel
Dresden University of Technology
Dresden, Germany

INTRODUCTION

During the last years numerical computation has been established as a powerful tool for investigation of flow and heat transfer in air-conditioned rooms. Nevertheless, there are some unsolved problems concerning evaluation of numerical data. The comparison of numerical results with experimental data is restricted to a relatively small number of investigated flow situations. Therefore, it is important to know which parameters (number of grid points, initial values, time step, weighting factors, etc.) considerably influence a numerical solution. Starting from a laminar flow in a simple model room, some situations are numerically investigated and evaluated. The research code "ResCUE" is used for the simulations. It is based on an explicit velocity-pressure iteration and a multigrid method. In terms of velocity, temperature and other transport quantities a combined one/two-step method is applied, the multigrid method is used to solve the Poisson equation for the pressure.

BASIC EQUATIONS, SOLUTION STRATEGY AND DISCRETIZATION

As basic equations we consider the time averaged transport equations for an incompressible fluid. By means of *Boussinesq's* eddy viscosity concept, *Boussinesq's* approximation of buoyancy and a k-ϵ turbulence model, the following system of differential equations is formed:

$$\frac{\partial \overline{U}_i}{\partial t} = \frac{\partial}{\partial x_j}\left(\nu_{eff}\left(\frac{\partial \overline{U}_i}{\partial x_j}+\frac{\partial \overline{U}_j}{\partial x_i}\right)\right) - \frac{\partial \overline{U}_j \overline{U}_i}{\partial x_j} - \frac{\partial \overline{P}}{\partial x_i} - g_i\gamma(\overline{T}-T_0), \qquad (1)$$

$$\frac{\partial \overline{U}_i}{\partial x_i} = 0, \tag{2}$$

$$\frac{\partial \overline{T}}{\partial t} = \frac{\partial}{\partial x_j}\left(a_{eff}\frac{\partial \overline{T}}{\partial x_j}\right) - \frac{\partial \overline{U}_j \overline{T}}{\partial x_j} + \overline{\dot{q}^V}, \tag{3}$$

$$\frac{\partial k}{\partial t} = \frac{\partial}{\partial x_j}\left(\left(\nu + \frac{\nu_t}{Pr_k}\right)\frac{\partial k}{\partial x_j}\right) - \frac{\partial \overline{U}_j k}{\partial x_j} + \nu_t \frac{\partial \overline{U}_i}{\partial x_j}\left(\frac{\partial \overline{U}_i}{\partial x_j} + \frac{\partial \overline{U}_j}{\partial x_i}\right) - \varepsilon + g_j \gamma \frac{\nu_t}{Pr_t}\frac{\partial \overline{T}}{\partial x_j}, \tag{4}$$

$$\frac{\partial \varepsilon}{\partial t} = \frac{\partial}{\partial x_j}\left(\left(\nu + \frac{\nu_t}{Pr_\varepsilon}\right)\frac{\partial \varepsilon}{\partial x_j}\right) - \frac{\partial \overline{U}_j \varepsilon}{\partial x_j} + C_1 \nu_t \frac{\varepsilon}{k}\frac{\partial \overline{U}_i}{\partial x_j}\left(\frac{\partial \overline{U}_i}{\partial x_j} + \frac{\partial \overline{U}_j}{\partial x_i}\right) - C_2 \frac{\varepsilon^2}{k} + C_1 g_j \gamma \frac{\nu_t}{Pr_t}\frac{\partial \overline{T}}{\partial x_j} \tag{5}$$

with

$$\overline{P} = \overline{p}/\rho, \tag{6}$$

$$\nu_{eff} = \nu + \nu_t, \tag{7}$$

$$a_{eff} = a + a_t, \tag{8}$$

$$\nu_t = C_D k^2/\varepsilon, \tag{9}$$

$$a_t = \nu_t / Pr_t. \tag{10}$$

In addition, appropriate initial and boundary conditions have to be specified. The set of constants of the turbulence model is shown in the table below.

C_D	C_1	C_2	Pr_t	Pr_ε	Pr_k
0,09	1,44	1,92	0,77	1,3	1,0

Instead of solving the fully discretized and linearized equation system (1)–(5) we use an explicit velocity–pressure iteration which is based on the algorithm of the Marker And Cell Method [1]. Our strategy of solution can be presented in the following manner:

• Integration of equation (1) and (3) over a time step and weighted approximation of the integrals:

$$\overline{U}_i^{m+1} = \overline{U}_i^m + \Delta t \left\{ \xi_1 \left[\frac{\partial}{\partial x_j}\left(\nu_{eff}\left(\frac{\partial \overline{U}_i}{\partial x_j} + \frac{\partial \overline{U}_j}{\partial x_i}\right)\right) - \frac{\partial \overline{U}_j \overline{U}_i}{\partial x_j} - \frac{\partial \overline{P}}{\partial x_i} - g_i \gamma (\overline{T} - T_0) \right]^m + \xi_2 \left[\frac{\partial}{\partial x_j}\left(\nu_{eff}\left(\frac{\partial \overline{U}_i}{\partial x_j} + \frac{\partial \overline{U}_j}{\partial x_i}\right)\right) - \frac{\partial \overline{U}_j \overline{U}_i}{\partial x_j} - \frac{\partial \overline{P}}{\partial x_i} - g_i \gamma (\overline{T} - T_0) \right]^{m-1} \right\} \tag{11}$$

$$\overline{T}^{m+1} = \overline{T}^m + \Delta t \left\{ \xi_1 \left[\frac{\partial}{\partial x_j}\left(a_{eff}\frac{\partial \overline{T}}{\partial x_j}\right) - \frac{\partial \overline{U}_j \overline{T}}{\partial x_j} + \overline{\dot{q}^V} \right]^m \right.$$

$$+\xi_2 \left[\frac{\partial}{\partial x_j} \left(a_{eff} \frac{\partial \overline{T}}{\partial x_j} \right) - \frac{\partial \overline{U}_j \overline{T}}{\partial x_j} + \overline{\dot{q}^V} \right]^{m-1} \Bigg\} \qquad (12)$$

with $\xi_1 = 1, \xi_2 = 0$ for the Euler method and $\xi_1 = 3/2, \xi_2 = -1/2$ for the two–step method of Adams–Bashforth.

- Analogous treatment of the equations (4) and (5).

- Calculation of pressure $\overline{P}^m$ using equation of mass conservation (2):

$$\begin{aligned} \frac{\partial^2 \overline{P}^m}{\partial x_i^2} &= \frac{1}{\xi_1 \Delta t} \frac{\partial \overline{U}_i^m}{\partial x_i} + \frac{\partial}{\partial x_i} \Bigg\{ \left[\frac{\partial}{\partial x_j} \left(\nu_{eff} \left(\frac{\partial \overline{U}_i}{\partial x_j} + \frac{\partial \overline{U}_j}{\partial x_i} \right) \right) - \frac{\partial \overline{U}_j \overline{U}_i}{\partial x_j} \right. \\ &\quad \left. - g_i \gamma (\overline{T} - T_0) \right]^m \qquad (13) \\ &+ \frac{\xi_2}{\xi_1} \left[\frac{\partial}{\partial x_j} \left(\nu_{eff} \left(\frac{\partial \overline{U}_i}{\partial x_j} + \frac{\partial \overline{U}_j}{\partial x_i} \right) \right) - \frac{\partial \overline{U}_j \overline{U}_i}{\partial x_j} - \frac{\partial \overline{P}}{\partial x_i} - g_i \gamma (\overline{T} - T_0) \right]^{m-1} \Bigg\}. \end{aligned}$$

(One can get boundary conditions for the pressure from equation (11).)

After calculating the pressure, new velocity, temperature and further transport quantities can be determined.

This explicit strategy is applicable both to steady and unsteady problems. The clearness of the algorithm is an advantage, i.e. every step of the algorithm is easy to understand and this strategy avoids the neglecting of any terms as it is done in other velocity–pressure iterations (e.g. [2]), but the restriction on the time step due to the explicit method is a disadvantage of it.

For the spatial discretization we employ a Finite Volume Method on a staggered grid. Simple upwind differences are used to discretize the convective terms. Some investgations concerning consistency and stability of the difference equations are presented in [3].

The linear equation system resulting from the discretization of the Poisson equation is solved by a multigrid method. By numerical studies we found out, that it is the best way to solve large difference equations systems, above all in terms of permanently increasing grid point numbers. We use a so called V–cycle with the Gauß–Seidel method as a smoothing iteration and the Cholesky method for solving the correction equation on the coarsest grid [4]. In case of uniform grids the contraction rate of this multigrid method (rate of reduction of the defect between two multigrid iteration steps) is nearly independent of the grid point number (e.g. see next section). But for calculation of flows in air conditioned rooms a uniform grid is unfavourable, because the supply opening is very small compared to the height of the room. To ensure the efficiency of the multigrid method, the simple Gauß–Seidel method is no longer a suitable smoothing iteration. At present we have been using a SOR iteration for smoothing, but it seems to be not the optimal one because the aspect ratio of the grid is restricted by approximately 1:3. Following the literature (e.g. [5]), a block iteration method does not suffer from the aspect ratio of the grid.

NUMERICAL INVESTIGATIONS AND RESULTS

We started our computations with a simple model room, see figure 1. In case of a la-

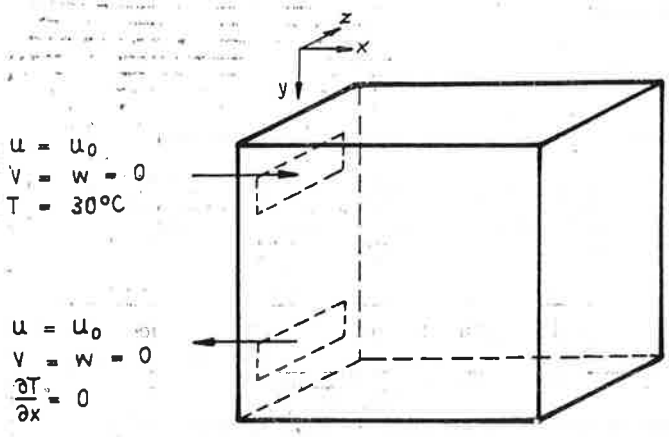

Figure 1: Geometry and boundary conditions of a simple 3D model room ($T_{wall} = 20°C, T_{backwall} = 30°C, T_{in} = 30°C$)

minar nonisothermal (uncoupled and coupled) situation (Re=205, Ar=1.16, Pr=0.7) we investigated the influence of the grid point number on the numerical solution. At the inlet, the outlet and the walls we applied Dirichlet boundary conditions for velocity. For temperature we used Dirichlet conditions, too, except at the outlet, where a homogeneous Neumann condition was given. The simulation was started with the flow at rest. Some results are shown in figures 2 and 3 and the next table. As it is shown by the figures the flow patterns of the 12^3 and 24^3 case are nearly identical. Nevertheless, there are some differences in predicting local properties.

Criterion / Computersimulation	12^3uncoup.	12^3coup.	24^3uncoup.	24^3coup.
Number of time steps	598	1113	1104	2040
Time step in [s]	0,053	0,053	0,024	0,024
Maximal velocity in [m/s]	0,071	0,079	0,072	0,083
Contractionrate of MG	0,049	0,045	0,051	0,048
Nußelt number back wall	5,6	15,3	8,3	19,6

The predicted maximal velocity in the inner flow domain is located in all cases near the inlet. It is shown, that the finer grid produces a higher velocity. The effort for the coupled solution is approximately twice as high as the effort for the uncoupled solution. The mean contraction rate of the multigrid method is nearly the same for all cases. The mean Nußelt number was calculated only at the hot back wall of the model room. The influence of the grid point number is considerably high compared to the influence of the maximal velocity. Generally we can state, that this two meshes show the different influence of the grid on various quantities. Nevertheless, more computations are necessary to recognize a clear tendency.

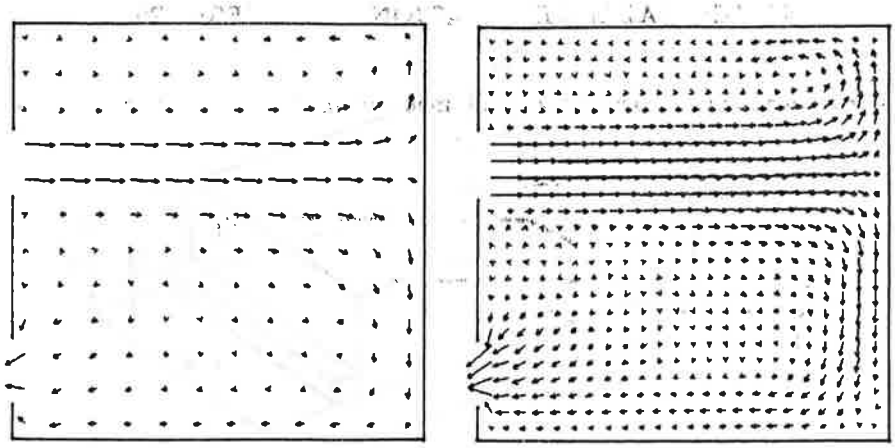

Figure 2: Velocity in the medium x–y–plane of the uncoupled case

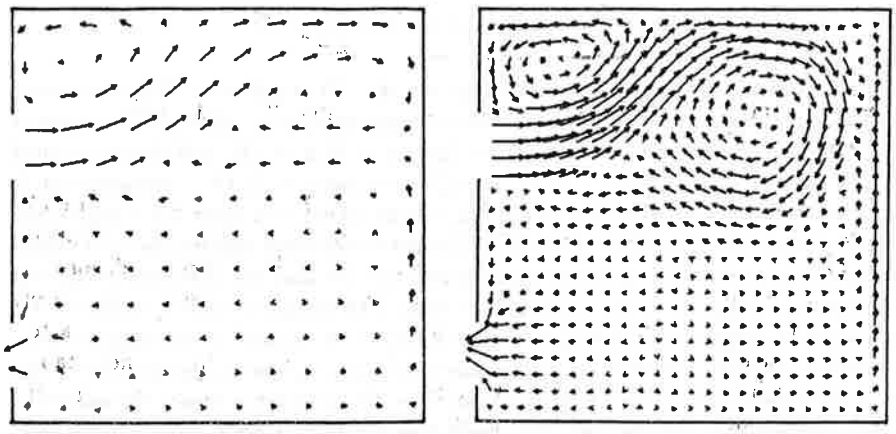

Figure 3: Velocity in the medium x–y–plane of the coupled case

It is almost impossible to get experimental data about such a situation, therefore we turned to another situation, which is well investigated from the experimental as well as the numerical point of view. We calculated the isothermal test case 2D1, proposed by *Nielsen* in 1990 [6]. The geometry of this test case is shown in figure 4. It is specified by the following values and boundary conditions at the inlet:

$$H = 3.0m, L = 9.0m, h = 0.168m, t = 0.48m \quad \text{and}$$
$$u_0 = 0.455m/s, k_0 = 1.5(0.04 \cdot u_0), \varepsilon_0 = C_D \cdot k_0^{1.5}/h/10.$$

Although that is a 2D test case, we calculated a quasi 2D and a 3D situation and assumed $W = 6.0m$. The simulations were carried out on a $64 \times 28 \times 4$ grid and symmetry conditions at the right and left wall for the 2D case and a $64 \times 28 \times 32$ grid for the 3D case. In contrast to the above presented simple model room the grid was non–uniform, in order to get enough grid lines at the inlet and the outlet. The simulations were started with a wall jet from the supply opening up to the opposite wall. A convereged solution was reached after about 6000 time steps for the 2D

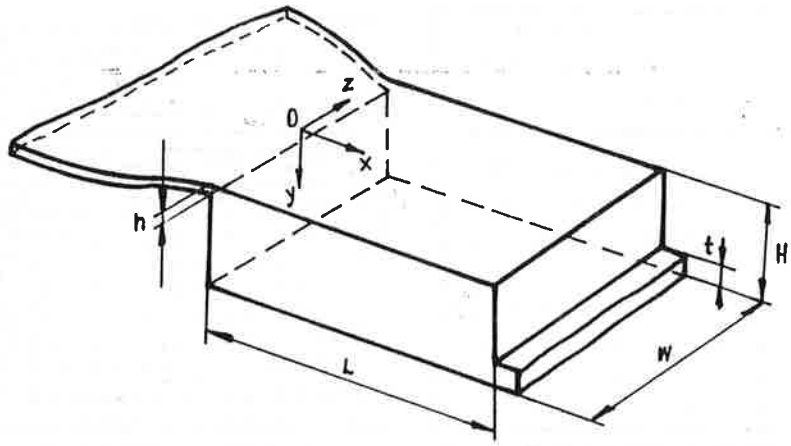

Figure 4: Geometry of the test case 2D1

simulation and after about 8000 time steps for the 3D simulation. The time step was approximately $0.05s$ in both calculations. Some results are shown in the figures 5–8. The profiles are given at the vertical lines $x = H, x = 2H$ and the horizontal lines $y = h/2, y = H - h/2$. The overall agreement with the measurement is good. Both predictions meet the characteristic situation and they are comparable with other numerical predictions (see [8]). Except some small regions the grid seems to be fine enough for this problem. Comparing the 2D and the 3D simulation, the results show an influence of the right and left wall. The assumed relation of $W/H = 2$ is too small to neglect the influence of the walls. It is shown by the figures, that the maximal velocity of the jet as well as the recirculating flow at the bottom of the room is overpredicted by the 3D simulation. The 2D simulation meets the values of the measurement in a satisfactory way. Both computations were carried out without relaxation of the turbulent quantities and without any damping of the production term. In this relatively simple situation no influence on the solution process was necessary.

A similar situation was investigated by *Hanel* [7]. The room was a small model with

$$H = 0.36m, L = 1.0m, h = 0.009m, t = 0.048m \quad \text{and}$$
$$u_0 = 4.3m/s, k_0 = 1.5(0.01 \cdot u_0), \varepsilon_0 = C_D \cdot k_0^{1.5}/h/10.$$

The quasi 2D simulation was carried out on a $128 \times 48 \times 4$ grid and was also started with a wall jet from the supply opening up to the opposite wall. It takes some 10000 time steps of approximately $0.0003s$ (nearly two days CPU–time on a HP 9000/730 workstation) to get a converged solution. Some results are shown in figure 9. Although the overall prediction of the flow pattern is satisfactory, there are some differences between measurement and numerical solution concerning the behaviour of the wall jet. The developement of the jet behind the supply opening is well predicted, but the further expansion of the jet was not represented by the

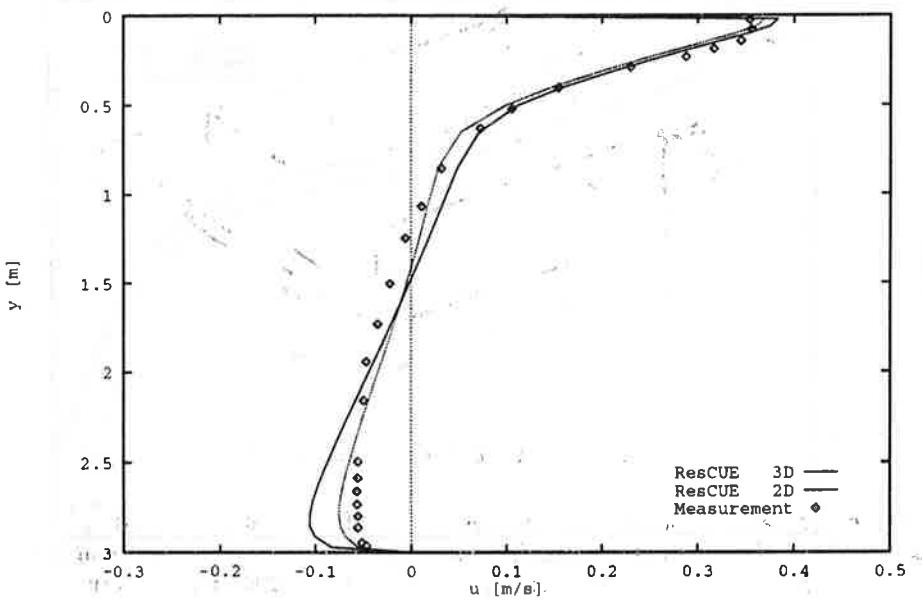

Figure 5: Measured and simulated velocity profiles at $x = H$ for the test case 2D1

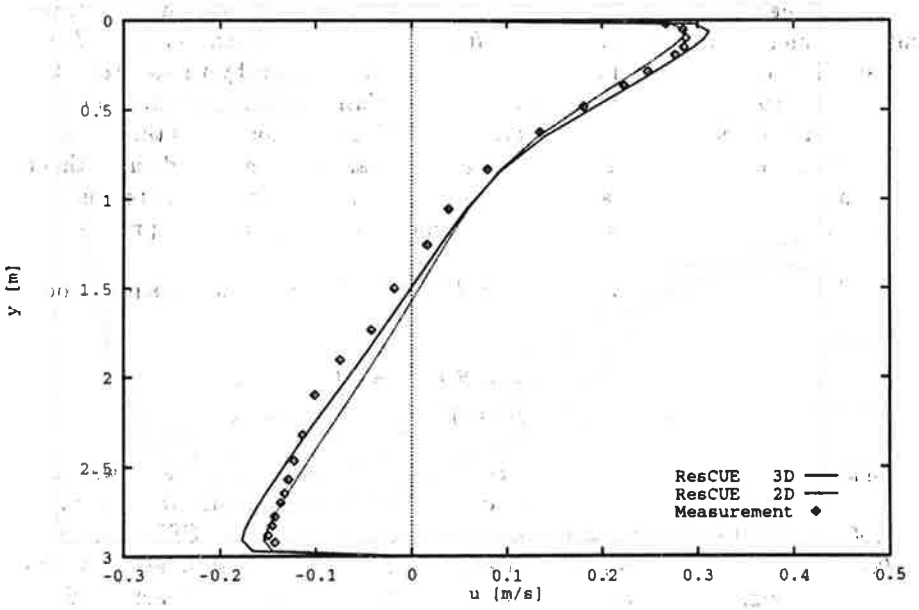

Figure 6: Measured and simulated velocity profiles at $x = 2H$ for the test case 2D1

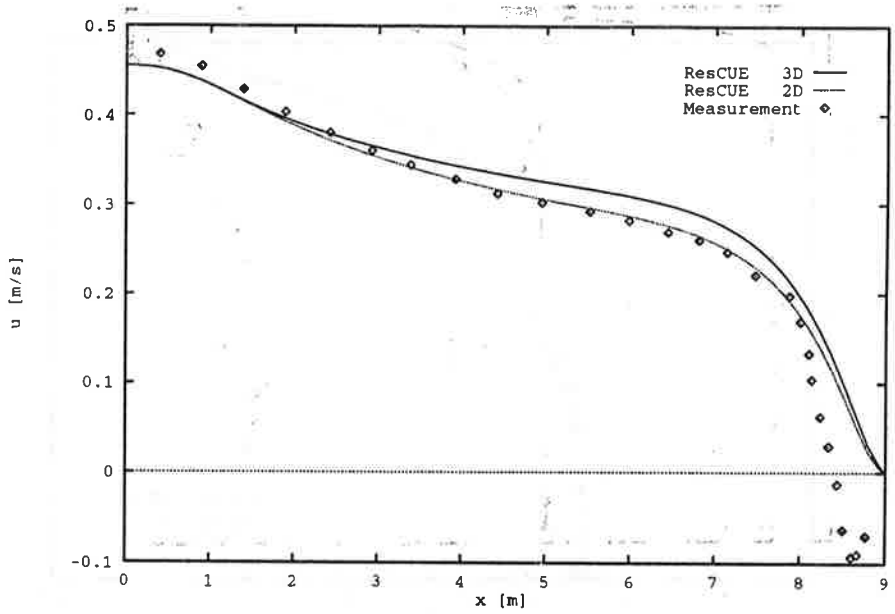

Figure 7: Measured and simulated velocity profiles at $y = h/2$ for the test case 2D1

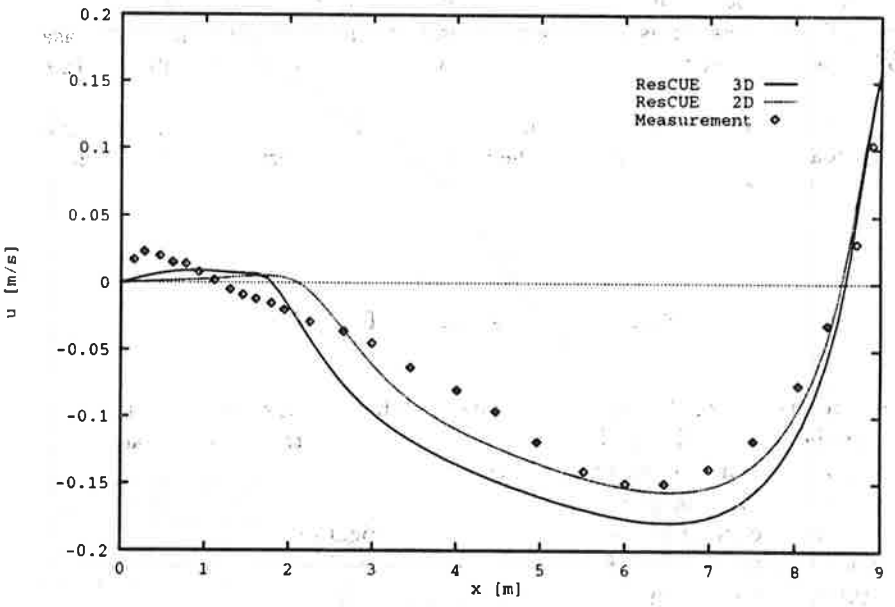

Figure 8: Measured and simulated velocity profiles at $y = H - h/2$ for the test case 2D1

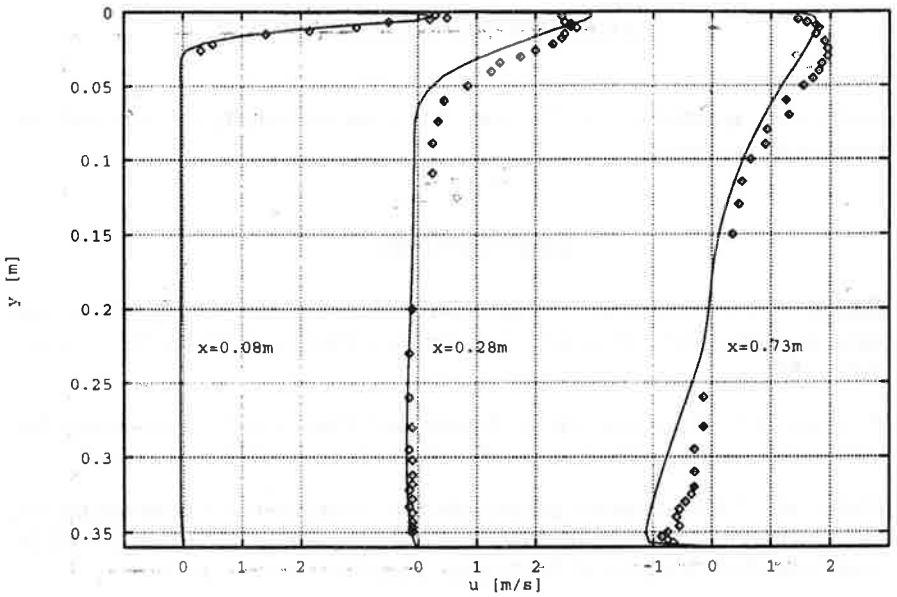

Figure 9: Measured and simulated velocity profiles at several vertical lines

calculation. The maximum velocity of the jet is displaced. Due to the relation $h/H = 0.025$ the situation is more complicated as in the above presented test case 2D1. The use of the standard k–ε model with wall functions is not suitable for this situation.

By numerical investigations we found out that in this case relaxation of the turbulent quantities and a damping of the production term during the first hundred time steps is favourable.

CONCLUSIONS AND OUTLOOK

The presented results of the simulations show the ability of the developed research code for predicting flows in ventilated rooms. The applied strategy is characterized by a high level of clearness and a robust behaviour. A critical point is the restriction of the time step, which leads to a very large number of time steps in case of very fine grids. To overcome this disadvantage, some investigations concerning the use of vector computers are planned. Furthermore, we want to implement a low Reynolds number turbulence model in order to improve the behaviour of the flow near the wall. In addition, numerical simulations of other flow situations (room with obstacle, steps and heat sources) in connection with experiments will be carried out.

ACKNOWLEDGEMENT

The authors are grateful to Mr. G. Morgenstern for his help by carrying out the numerous computations.

REFERENCES

[1] Harlow F. H.; Welch J. E. "Numerical calculation of time dependent viscous incompressible flow of fluid with free surface". Physics of Fluids, 8, 1965, pp. 2182-2189.

[2] Patankar, S.V. "Numerical Heat Transfer and Fluid Flow". Hemisphere Publishing Corporation, Washington, New York, London 1982

[3] Rösler, M. "Mathematisch–numerische Untersuchungen zur Berechnung von dreidimensionalen, inkompressiblen Kanal–und Raumluftströmungen". Ph.D. thesis Dresden University of Technology, Dresden, 1992.

[4] Hanel, B.; Rösler, M. "Multigrid–Application for the Solution of Large Difference Equation Systems". IEA–paper of ANNEX 20: Air Flow Patterns within Buildings, 12th AIVC Conference, 1991

[5] Brandt, A. "Multi-level adaptive solutions to boundary-value problems". Mathematics of Computation 13, 1977, pp.333–390

[6] Nielsen, P.V. "Specification of a two-dimensional test case". ANNEX 20 - Internal report, Aalborg, 1990.

[7] Scholz, R.; Hanel, B. "Computergestützte Berechnung der Raumluftströmung". Verlag Technik, Berlin, 1988.

[8] Whittle, G. E. "Evaluation of measured and computed test case, results from ANNEX 20, subtask 1". 12th AIVC Conference, Air Movement & Ventilation Control within Buildings, Ottawa, 1991.